

# Dynamical phase transition in correlated fermionic lattice systems

Martin Eckstein,<sup>1</sup> Marcus Kollar,<sup>1</sup> and Philipp Werner<sup>2</sup>

<sup>1</sup>*Theoretical Physics III, Center for Electronic Correlations and Magnetism,  
Institute for Physics, University of Augsburg, 86135 Augsburg, Germany*

<sup>2</sup>*Theoretical Physics, ETH Zurich, 8093 Zurich, Switzerland*

(Dated: April 6, 2009)

We use non-equilibrium dynamical mean-field theory to demonstrate the existence of a critical interaction in the real-time dynamics of the Hubbard model after an interaction quench. The critical point is characterized by fast thermalization and separates weak-coupling and strong-coupling regimes in which the relaxation is delayed due to prethermalization on intermediate timescales. This dynamical phase transition should be observable in experiments on trapped fermionic atoms.

PACS numbers: 67.40.Fd, 71.10.Fd, 05.10.Ln

The properties of correlated many-particle systems can change dramatically and abruptly as external parameters are varied. An important example is the Mott transition from an itinerant state to a correlation-induced insulator, which occurs in such diverse systems as transition-metal compounds [1] and ultracold quantum gases [2, 3, 4]. An entirely new perspective on those systems is provided by their nonequilibrium dynamics after an external perturbation, which is experimentally accessible not only in the case of well-controlled ultracold quantum gases, but also for electrons in solids by means of femtosecond spectroscopy [5, 6, 7, 8, 9]. On short timescales the perturbed systems are essentially decoupled from the environment and follow the unitary time evolution according to the Schrödinger equation, which immediately raises a number of questions: How does an isolated many-body system approach a new equilibrium after being quenched, i.e., after a sudden change in one of its parameters? Does it eventually thermalize, or is detailed memory on the initial state retained for all times?

Recently these questions have been addressed in a number of experimental [10, 11] and theoretical investigations [12, 13, 14, 15, 16, 17, 18, 19, 20, 21]. After a quench to a large interaction parameter  $U$  characteristic collapse-and-revival oscillations with period  $2\pi\hbar/U$  appear, which are due to the integer eigenvalues of the interaction operator [2, 12, 14, 15, 16, 19, 20, 21, 22]. These oscillations eventually fade out, but in some cases the system is trapped in a nonthermal stationary state up to the largest accessible times [14, 15]. At first glance this may seem surprising because thermalization is only known to be inhibited for integrable systems [12, 13, 19], whereas nonintegrable systems such as those studied in Refs. 14, 15 are expected to thermalize [17]. Nonthermal quasistationary states are found, on the other hand, on an intermediate timescale ( $\propto 1/U^2$ ) after quenches to small interaction parameters [18]; the prethermalization to these states is followed by an approach to thermal equilibrium on a much longer timescale ( $\propto 1/U^4$ ). Another interesting observation is that the relaxation dynamics can depend sensitively on the parameters of the final

Hamiltonian [21]. Whether and how this phenomenon, which may be called a dynamical phase transition, relates to the existence of an equilibrium thermodynamic phase transition, remains to be clarified.

Here we consider the relaxation of correlated lattice fermions described by a time-dependent Hubbard Hamiltonian at half-filling,

$$H(t) = \sum_{ij\sigma} V_{ij} c_{i\sigma}^\dagger c_{j\sigma} + U(t) \sum_i (n_{i\uparrow} - \frac{1}{2})(n_{i\downarrow} - \frac{1}{2}), \quad (1)$$

using nonequilibrium dynamical mean-field theory (DMFT). We restrict ourselves to the paramagnetic phase and choose hoppings  $V_{ij}$  corresponding to a semi-elliptic density of states  $\rho(\epsilon) = \sqrt{4V^2 - \epsilon^2}/(2\pi V)$ . The system is initially in the ground state of the noninteracting Hamiltonian, i.e.,  $U(t < 0) = 0$ . At  $t = 0$  the Coulomb repulsion is switched to a finite value,  $U(t \geq 0) = U$ . Energy is measured in units of the quarter-bandwidth  $V$  and time in units of  $1/V$ , i.e., we set  $\hbar = 1$  and in the figures also  $V = 1$ . Our results confirm the prethermalization for quenches to  $U \ll V$  and indicate a second prethermalization regime for  $U \gg V$ , for which we provide a general perturbative argument. At  $U_c^{\text{dyn}} = 3.2V$  we observe a sharp crossover between the two regimes, suggestive of a dynamical phase transition in the above sense.

*Nonequilibrium DMFT.*— In equilibrium DMFT, which becomes exact in the limit of infinite dimensions [23], the self-energy is local and can be calculated from a single-site impurity model subject to a self-consistency condition [24]. Nonequilibrium DMFT is a reformulation for Green functions on the Keldysh contour [25, 26], which maps the lattice problem (1) onto a single-site problem described by the action

$$\mathcal{S} = \sum_{\sigma=\uparrow,\downarrow} \int_C dt dt' c_\sigma^\dagger(t) \Lambda_\sigma(t, t') c_\sigma(t') + \int_C dt h_{\text{loc}}(t), \quad (2)$$

where  $h_{\text{loc}}(t) = U(t)[n_\uparrow(t) - \frac{1}{2}][n_\downarrow(t) - \frac{1}{2}]$  is the local Hamiltonian at half-filling. For a system that is prepared in equilibrium with temperature  $T$  at times  $t$

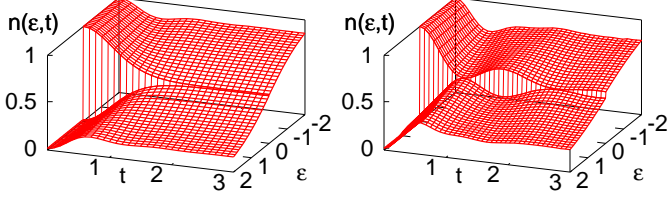


FIG. 1: Momentum distribution  $n(\epsilon_{\mathbf{k}}, t)$  for quenches from  $U = 0$  to  $U = 3$  (left panel) and  $U = 5$  (right panel).

$< 0$  the time-contour  $\mathcal{C}$  is chosen to run from  $t = 0$  along the real axis to  $t_{\max}$ , back to 0, and finally to  $-i/T$  along the imaginary axis. The action  $\mathcal{S}$  determines the contour-ordered Green function  $G_{\sigma}(t, t') = \text{Tr}[T_{\mathcal{C}} e^{-i\mathcal{S}} c_{\sigma}(t) c_{\sigma}^{\dagger}(t')]/Z$  and the self-energy  $\Sigma(t, t')$ . For the semi-elliptic density of states the selfconsistency condition reduces to  $\Lambda_{\sigma}(t, t') = V^2 G_{\sigma}(t, t')$  [16]. The single-site problem can be solved, for example, by means of real-time Monte Carlo techniques [27, 28]. We use the weak-coupling continuous-time Monte Carlo (CTQMC) algorithm [28], which stochastically samples a diagrammatic expansion in powers of the interaction part  $h_{\text{loc}}$  and measures observables such as the local Green function  $G_{\sigma}(t, t')$ . The weak-coupling method is highly suitable for initial noninteracting states, because the imaginary branch of the contour does not enter the CTQMC calculation. This allows us to study initial states at zero temperature by transforming imaginary times to real frequencies. Furthermore, the parameters of the algorithm can be chosen such that only even orders contribute to  $G_{\sigma}(t, t')$  at half-filling, which reduces the sign problem. Computational details are deferred to a separate publication.

Many observables of the lattice model can be calculated from the local Green function  $G_{\sigma}(t, t')$  and the self-energy  $\Sigma_{\sigma}(t, t')$ . The two-particle correlation function  $\Gamma_{\sigma}(t, t') = \langle T_{\mathcal{C}} c_{i\sigma}^{\dagger}(t) [n_{i\bar{\sigma}}(t) - \frac{1}{2}] c_{i\sigma}(t') \rangle$  is obtained from the contour convolution  $\Gamma_{\sigma} = G_{\sigma} * \Sigma_{\sigma}$  and yields the double occupation  $d(t) = \langle n_{i\uparrow}(t) n_{i\downarrow}(t) \rangle$  at  $t = t'$ . (Local quantities do not depend on the site index  $i$  for the homogeneous phase.) Solving the the lattice Dyson equation  $(i\partial_t + \mu - \epsilon - \Sigma_{\sigma}) * G_{\epsilon\sigma} = 1$  yields the momentum-resolved equal-time Green function  $G_{\epsilon\sigma}(t, t)$  and thus the momentum distribution  $n(\epsilon_{\mathbf{k}}, t) = \langle c_{\mathbf{k}\sigma}^{\dagger}(t) c_{\mathbf{k}\sigma}(t) \rangle$ , as well as the kinetic energy per lattice site,  $E_{\text{kin}}(t)/L = 2 \int d\epsilon \rho(\epsilon) n(\epsilon, t) \epsilon$ . The total energy  $E = E_{\text{kin}}(t) + UL[d(t) - 1/4]$  must be conserved after the quench, and we use this as a check for the numerical solution.

*Results.* — As depicted in Fig. 1, the momentum distribution  $n(\epsilon, t)$  evolves from a step function in the initial state to a continuous function of  $\epsilon$  at large times. Remarkably, its discontinuity at  $\epsilon = 0$ , which marks the

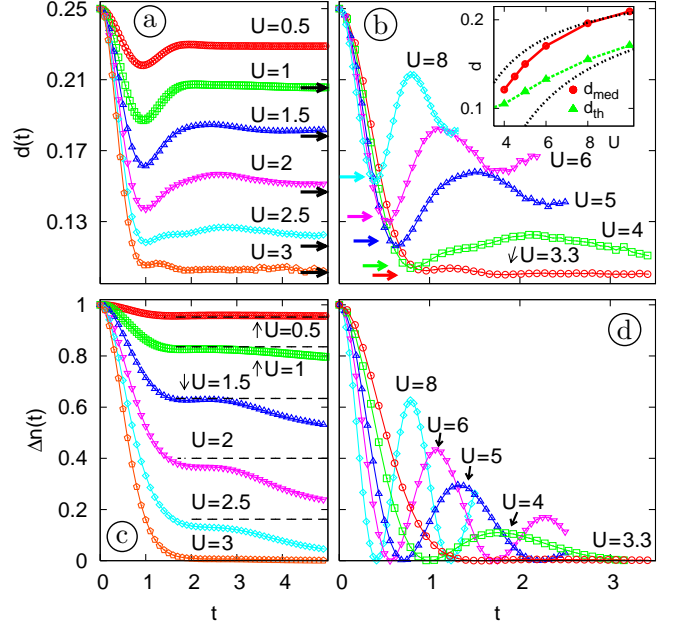


FIG. 2: Fermi surface discontinuity  $\Delta n$  and double occupation  $d(t)$  after quenches to  $U \leq 3$  (left panels) and  $U \geq 3.5$  (right panels). Horizontal dotted lines in the upper left panel are at the quasistationary value  $\Delta n_{\text{stat}} = 2Z - 1$  predicted in Ref. 18, with the  $T = 0$  quasiparticle weight  $Z$  taken from equilibrium DMFT data [30]. Horizontal arrows indicate corresponding thermal values  $d_{\text{th}}$  of the double occupation, obtained from equilibrium DMFT using QMC. Inset: thermal value  $d_{\text{th}}$  and  $d_{\text{med}}$ , the average of the first maximum and the second minimum of  $d(t)$ , which provides an estimate of the stationary value  $d_{\text{stat}}$ ; black dotted lines are the respective results from the strong-coupling expansion (see text).

Fermi surface in the initial state, remains sharp while its height decays smoothly to zero. For a noninteracting initial state at half-filling, the discontinuity  $\Delta n(t) = n(0^-, t) - n(0^+, t)$  can be expressed as

$$\Delta n(t) = |G_{\epsilon=0, \sigma}^{\text{ret}}(t, 0)|^2, \quad (3)$$

where  $G_{\epsilon_{\mathbf{k}\sigma}}^{\text{ret}}(t, 0) = -i\Theta(t)\langle \{c_{\mathbf{k}\sigma}(0), c_{\mathbf{k}\sigma}^{\dagger}(t)\} \rangle$  is the retarded component of the momentum-resolved Green function. This shows that the collapse of the discontinuity  $\Delta n$  is closely related to the decay of electron and hole excitations which are created at time  $t = 0$  at the Fermi surface.

We now use  $\Delta n(t)$  and  $d(t)$  to characterize the relaxation after the quench. As shown in detail below, these functions behave qualitatively different in the weak-coupling and strong-coupling regimes, separated by a very sharp crossover at  $U_c^{\text{dyn}} = 3.2V$ . We test for thermalization by comparing to expectation values in a grand-canonical ensemble with the same total energy.

*Weak-coupling regime,  $U < U_c^{\text{dyn}}$ .* — For quenches to  $U \leq 3V$  (Fig. 2a,c) we find that the double occupation  $d(t)$  relaxes from its initial uncorrelated value  $d(0) =$

$\langle n_\uparrow \rangle_0 \langle n_\downarrow \rangle_0 = 1/4$  [29] almost to its thermal value  $d_{\text{th}}$ , while the Fermi surface discontinuity  $\Delta n(t)$  remains finite for times  $t \leq 5/V$ . This confirms the predictions by Moeckel and Kehrein [18] of a quasistationary state which is formed on timescales on the order of  $V/U^2$  and has  $d_{\text{stat}} = d_{\text{th}} + \mathcal{O}(U^3/V^3)$  and finite  $\Delta n_{\text{stat}} = 1 - 2Z$ . Here  $Z$  is the quasiparticle weight in equilibrium at zero temperature and interaction  $U$ . Their prediction was based on a perturbative flow equation analysis for  $U \ll V$  and it was argued that full thermalization occurs only on much longer timescales on the order of  $V^3/U^4$ . At  $t = 2/V$  our numerical data agree very well with the predicted value of  $\Delta n_{\text{stat}}$  for  $U \leq 1V$ . Note that even for quenches to larger  $U$ , a prethermalization plateau remains visible in Fig. 2c at roughly this value, although the timescales  $V/U^2$  and  $V^3/U^4$  are no longer well separated.

*Strong-coupling regime,  $U > U_c^{\text{dyn}}$ .*— For quenches to large  $U$  we observe collapse-and-revival oscillations with approximate frequency  $2\pi/U$  both in  $d(t)$  and  $\Delta n(t)$  (Fig. 2b,d). This phenomenon is well understood in the atomic limit ( $V = 0$ ), where the propagator  $e^{-iHt}$  is exactly  $2\pi/U$ -periodic [2]. As expected, these oscillations are damped for nonzero  $V$ : at least for small times, they fall off on timescales on the order of  $1/V$ . Interestingly, the first few oscillations of  $d(t)$  are not centered around the thermal value  $d_{\text{th}}$  (solid arrows in Fig. 2b), which is instead located close to the first minimum of  $d(t)$ . This suggests a prethermalization regime also for  $U \gg V$ , as discussed in Ref. 14, where oscillations in  $d(t)$  are damped to a nonthermal quasistationary value on the timescale  $1/V$ , while full thermalization can only happen on the longer timescale  $U/V^2$ .

We now show that this prethermalization regime is a general feature of fermionic Hubbard-type models at strong coupling and calculate the double occupation in the quasistationary state. We use the standard unitary transformation  $\bar{A} = e^{-S} A e^S$  [31] for which the double occupation  $\bar{D} = \sum_i \bar{n}_{i\uparrow} \bar{n}_{i\downarrow}$  of the dressed fermions  $\bar{c}_{i\sigma}$  is conserved,  $[H, \bar{D}] = 0$ . After decomposing the hopping term [32],  $K = \sum_{ij\sigma} (V_{ij\sigma}/V) c_{i\sigma}^\dagger c_{j\sigma}$ , into parts  $K_p$  that change the double occupation by  $p$ , i.e.,  $K_+ = \sum_{ij\sigma} (V_{ij\sigma}/V) c_{i\sigma}^\dagger c_{j\sigma} (1 - n_{j\bar{\sigma}}) n_{i\bar{\sigma}} = (K_-)^+$  and  $K_0 = K - K_+ - K_-$ , the leading order transformation is  $S = (V/U)\bar{K}_+ + (V/U)^2[\bar{K}_+, \bar{K}_0] - \text{h.c.} + \mathcal{O}(V^3/U^3)$ . For the double occupation,  $d(t) = \langle e^{iHt} D e^{-iHt} \rangle_0 / L$ , we obtain

$$d(t) = d_{\text{stat}} - \frac{2V}{U} \text{Re} [e^{itU} R(tV)] + \mathcal{O}\left(\frac{V^2}{U^2}, \frac{tV^3}{U^2}\right), \quad (4)$$

where  $R(tV) = \langle e^{itVK_0} K_+ e^{-itVK_0} \rangle_0 / L$  and  $d_{\text{stat}} = d(0) + (2V/U) \text{Re} \langle K_+ / L \rangle_0$ . The error  $\mathcal{O}(tV^3/U^2)$ , which is due to omitted terms in the exponentials  $e^{\pm iHt}$ , is irrelevant in comparison to the leading terms if  $t \ll U/V^2$ . It remains to show that (i) the envelope function  $R(tV)$  of the oscillating term decays to zero for  $t \gg 1/V$ , and (ii) the quasistationary value  $d_{\text{stat}}$  differs from the ther-

mal value  $d_{\text{th}}$ . (i) Inserting an eigenbasis  $K_0|m\rangle = k_m|m\rangle$  yields  $R(tV) = \sum_{m,n} \langle |n\rangle \langle m| \rangle_0 e^{itV(k_m - k_n)} \langle n|K_+|m\rangle$ . In this expression all oscillating terms dephase in the long-time average [17, 19], so that only energy-diagonal terms contribute to the sum. But from  $[K_0, D] = 0$  it follows that  $D$  is a good quantum number of  $|n\rangle$  so that  $\langle n|K_+|n\rangle = 0$ , and thus  $R(tV)$  vanishes in the long-time limit (if it exists and if accidental degeneracies between sectors of different  $D$  are irrelevant). From Eq. (4) we therefore conclude that  $d(t)$  equals  $d_{\text{stat}}$  for times  $1/V \ll t \ll U/V^2$ , up to corrections of order  $\mathcal{O}(V^2/U^2)$ . (ii) For the quasistationary value  $d_{\text{stat}}$  we obtain

$$d_{\text{stat}} = d(0) - \Delta d, \quad (5a)$$

$$\Delta d = - \sum_{ij\sigma} \frac{V_{ij\sigma}}{UL} \langle c_{i\sigma}^\dagger c_{j\sigma} (n_{i\bar{\sigma}} - n_{j\bar{\sigma}})^2 \rangle_0, \quad (5b)$$

which applies to arbitrary initial states. For noninteracting initial states the expectation value in this expression factorizes; in DMFT Eq. (5b) then evaluates to  $\Delta d = n(1 - n/2)(V/U) \langle K/L \rangle_0$ , i.e., it is proportional to the kinetic energy in the initial state. For the thermal value  $d_{\text{th}}$  we expand the free energy in  $V/T_*$ , because the effective temperature  $T_*$  is much larger than  $V$  after a quench to  $U \gg V$ . At half-filling we obtain  $d_{\text{th}} = d(0) + (V/U) \langle K/L \rangle_0$ ; for noninteracting initial states in DMFT we thus find that  $\Delta d = d(0) - d_{\text{stat}} = [d(0) - d_{\text{th}}]/2$ , i.e., at times  $1/V \ll t \ll U/V^2$  the double occupation has relaxed only halfway towards  $d_{\text{th}}$ .

The strong-coupling predictions for the prethermalization plateau agree with our numerical results, for which the center of the first oscillation in  $d(t)$  approaches  $d_{\text{stat}}$  for large  $U$  (inset in Fig. 2b). The scenario also applies to interaction quenches in the half-filled Falicov-Kimball model in DMFT [16] and the  $1/r$  Hubbard chain [19], although thermalization is inhibited in these models: in both models the long-time limit of  $d(t \rightarrow \infty)$  can be obtained exactly and indeed agrees with  $d_{\text{stat}}$  for  $U \gg V$ . For quenches to large  $U$  in the free  $1/r$  chain (with bandwidth  $2\pi V$ ) Eq. (5b) yields  $\Delta d = (V/U)(1 - 2n/3)\pi$ . For the Falicov-Kimball model  $\Delta d$  is half as big as for the Hubbard model because only one spin species contributes to the kinetic energy in the initial state.

*Critical region,  $U \approx U_c^{\text{dyn}} = 3.2V$ .*— The characteristic collapse-and-revival oscillations of the strong-coupling regime disappear for quenches to  $U$  between  $3.3V$  and  $3V$ , as is apparent from the Fermi surface discontinuity  $\Delta n_1$  at its first revival maximum (Fig. 3a). This change in the short-time dynamics reflects a change in the nature of single-particle excitations [Eq. (3)]. It occurs also in equilibrium even at very high temperatures, because  $|G_{e\sigma}^{\text{ret}}(t - t')|^2$  becomes oscillatory upon the transfer of spectral weight to the Hubbard subbands at  $\pm U$ . Additionally the prethermalization plateau at  $\Delta n_{\text{stat}}$  disappears between  $3V$  and  $3.3V$ , so that the system can relax rapidly after quenches to  $U$  values in this range: momen-

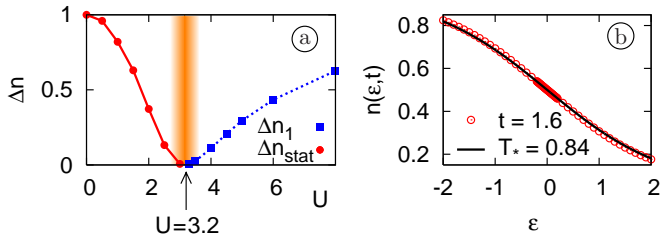


FIG. 3: Left panel:  $U$ -dependence of the prethermalization plateau,  $\Delta n_{\text{stat}}$ , and the first revival maximum,  $\Delta n_1$ , suggesting a dynamical phase transition at  $U_c^{\text{dyn}} = 3.2V$ . Right panel: momentum distribution at time  $t = 1.6$  after a quench to  $U = 3.3V$ ; the momentum distribution has essentially thermalized. The shaded area marks the critical region near  $U_c^{\text{dyn}} = 3.2V$  with very fast thermalization.

tum distribution and double occupation reach their respective thermal values already before the first expected collapse-and-revival oscillation at time  $2\pi/U$  (Fig. 3b). This suggests that the prethermalization regimes at weak and strong Hubbard interaction are separated by a special point, which we estimate from our data to be located at  $U_c^{\text{dyn}} = 3.2V$ , where relaxation processes on all energy scales become relevant. This sharp crossover is quite remarkable in view of the fact that the effective temperature  $T_*$  after the quench is much higher than the critical endpoint of the Mott metal-insulator transition in equilibrium ( $T_c \approx 0.055V$  [24], whereas  $T_* = 0.84V$  for  $U = 3.3V$ ), so that in equilibrium metallic and insulating phases could hardly be distinguished. A similar critical behavior was found for quenches in Heisenberg chains [21]. Therefore one might speculate that such *dynamical phase transitions* are a generic property of the nonequilibrium dynamics of correlated systems; however, this issue requires further study. In particular it would be interesting to see whether there is also an abrupt change in the long-time behavior at the same  $U_c^{\text{dyn}}$ .

*Conclusion.*— We determined the real-time dynamics of the Hubbard model after a quench from the noninteracting state using nonequilibrium DMFT, for which CTQMC [27, 28] proves to be a very suitable impurity solver. This method allows to investigate the transient dynamics of correlated fermions in a variety of contexts, e.g., to describe experiments with cold atomic gases [3, 4] or pump-probe spectroscopy on correlated electrons [16]. For the Hubbard model we found that rapid thermalization occurs after quenches to  $U \approx U_c^{\text{dyn}}$ ; in fact this is one of the few cases [14, 17] where thermalization can be numerically observed for a non-integrable model. On the other hand, for quenches to very small or very large interactions, the system becomes trapped in quasistationary states on intermediate timescales. The phenomena discussed in this paper are manifest in the momentum distribution and double occupation; both quantities are directly accessible in experiments with cold atomic gases.

We thank S. Kehrein, C. Kollath, M. Moeckel, M. Punk, M. Rigol, A. Silva, and D. Vollhardt for useful discussions. M.E. acknowledges support by Studienstiftung des deutschen Volkes. This work was supported in part by SFB 484 of the Deutsche Forschungsgemeinschaft (M.E., M.K.) and grant PP002-118866 of the Swiss National Science Foundation (P.W.). CTQMC calculations were run on the Brutus cluster at ETH Zurich, using the ALPS library [33].

- 
- [1] M. Imada *et al.*, Rev. Mod. Phys. **70**, 1039 (1998).
  - [2] M. Greiner *et al.*, Nature **415**, 39 (2002); M. Greiner *et al.*, Nature **419**, 51 (2002).
  - [3] R. Jördens *et al.*, Nature **455**, 204 (2008).
  - [4] U. Schneider *et al.*, Science **322**, 1520 (2008).
  - [5] T. Ogasawara *et al.*, Phys. Rev. Lett. **85**, 2204 (1000).
  - [6] S. Iwai *et al.*, Phys. Rev. Lett. **91**, 057401 (2003).
  - [7] L. Perfetti *et al.*, Phys. Rev. Lett. **97**, 067402 (2006); L. Perfetti *et al.*, New J. Phys. **10**, 053019 (2008).
  - [8] H. Okamoto *et al.*, Phys. Rev. Lett. **98**, 037401 (2007).
  - [9] C. Kübler *et al.*, Phys. Rev. Lett. **99**, 116401 (2007).
  - [10] T. Kinoshita *et al.*, Nature **440**, 900 (2006).
  - [11] S. Hofferberth *et al.*, Nature **449**, 324 (2007).
  - [12] M. Rigol *et al.*, Phys. Rev. Lett. **98**, 050405 (2007); M. Rigol *et al.*, Phys. Rev. A, **74**, 053616 (2006).
  - [13] M. A. Cazalilla, Phys. Rev. Lett. **97**, 156403 (2006); A. Iucci and M. A. Cazalilla, arXiv:0903.1205 (unpublished).
  - [14] C. Kollath *et al.*, Phys. Rev. Lett. **98**, 180601 (2007).
  - [15] S. R. Manmana *et al.*, Phys. Rev. Lett. **98**, 210405 (2007).
  - [16] M. Eckstein and M. Kollar, Phys. Rev. Lett. **100**, 120404 (2008); Phys. Rev. B **78**, 205119 (2008); *ibid.*, 245113.
  - [17] M. Rigol *et al.*, Nature **452**, 854 (2008).
  - [18] M. Möckel and S. Kehrein, Phys. Rev. Lett. **100**, 175702 (2008); arXiv:0903.1561 (unpublished).
  - [19] M. Kollar and M. Eckstein, Phys. Rev. A **78**, 013626 (2008).
  - [20] D. Rossini *et al.*, Phys. Rev. Lett. **102**, 127204 (2009).
  - [21] P. Barnettler *et al.*, arXiv:0810.4845 (unpublished).
  - [22] O. V. Misochko *et al.*, Phys. Rev. Lett. **92**, 197401 (2004).
  - [23] W. Metzner and D. Vollhardt, Phys. Rev. Lett. **62**, 324 (1989).
  - [24] A. Georges *et al.*, Rev. Mod. Phys. **68**, 13 (1996).
  - [25] P. Schmidt and H. Monien, arXiv:cond-mat/0202046 (unpublished);
  - [26] J. K. Freericks *et al.*, Phys. Rev. Lett. **97**, 266408 (2006).
  - [27] L. Mühlbacher and E. Rabani, Phys. Rev. Lett. **100**, 176403 (2008).
  - [28] P. Werner *et al.*, Phys. Rev. B **79**, 035320 (2009).
  - [29] Here and throughout the subscript 0 denotes expectation values in the initial state at time  $t = 0$ .
  - [30] R. Bulla, Phys. Rev. Lett. **83**, 136 (1999).
  - [31] A. B. Harris and R. V. Lange, Phys. Rev. **157**, 295 (1967).
  - [32] The derivation holds for arbitrary (and possibly spin-dependent) hopping  $V_{ij\sigma}$ .
  - [33] A. F. Albuquerque *et al.*, Journal of Magnetism and Magnetic Materials **310**, 1187 (2007).